


Research Article

# Preferential adsorption to air–water interfaces: a novel cryoprotective mechanism for LEA proteins

Fanny Yuen<sup>1,\*†</sup>, Matthew Watson<sup>1,†‡</sup>, Robert Barker<sup>2,§</sup>, Isabelle Grillo<sup>2</sup>, Richard K. Heenan<sup>3</sup>, Alan Tunnacliffe<sup>1</sup> and  Alexander F. Routh<sup>1</sup>

<sup>1</sup>Department of Chemical Engineering and Biotechnology, University of Cambridge, Philippa Fawcett Drive, Cambridge CB3 0AS, U.K.; <sup>2</sup>Institut Laue Langevin, 38042 Grenoble, Cedex 9, France; <sup>3</sup>SIS Facility, Science & Technology Facilities Council, Rutherford Appleton Laboratory, Chilton, Oxon OX11 0QX, U.K.

Correspondence: Alexander F. Routh (afr10@cam.ac.uk)



Late embryogenesis abundant (LEA) proteins comprise a diverse family whose members play a key role in abiotic stress tolerance. As intrinsically disordered proteins, LEA proteins are highly hydrophilic and inherently stress tolerant. They have been shown to stabilise multiple client proteins under a variety of stresses, but current hypotheses do not fully explain how such broad range stabilisation is achieved. Here, using neutron reflection and surface tension experiments, we examine in detail the mechanism by which model LEA proteins, AavLEA1 and ERD10, protect the enzyme citrate synthase (CS) from aggregation during freeze–thaw. We find that a major contributing factor to CS aggregation is the formation of air bubbles during the freeze–thaw process. This greatly increases the air–water interfacial area, which is known to be detrimental to folded protein stability. Both model LEA proteins preferentially adsorb to this interface and compete with CS, thereby reducing surface-induced aggregation. This novel surface activity provides a general mechanism by which diverse members of the LEA protein family might function to provide aggregation protection that is not specific to the client protein.

## Introduction

Late embryogenesis abundant (LEA) proteins comprise a diverse family of intrinsically disordered proteins (IDPs) that are thought to play a key role in tolerance to abiotic stresses such as freezing and desiccation. These proteins are of particular interest because of their link to advancement in stress-tolerant technologies and the development of novel biomedical preservation techniques. Originally identified almost 40 years ago in cotton seed embryos, LEA genes have since been found in a variety of different organisms, where their presence and expression correlates with the acquisition of stress tolerance (for reviews, see refs [1–3]). LEA proteins are highly variable in sequence, molecular mass and charge, and have been classified into 12 different groups [4]. However, there is no evidence that members of any particular group carry out distinct functions *in vivo*. As IDPs, LEA proteins are hydrophilic and contain little or no secondary structure. This makes LEA proteins inherently tolerant to conditions that denature folded proteins, and they are thought to stabilise folded cellular proteins under conditions of abiotic stress. Several hypotheses have been proposed regarding the function of LEA proteins in stress tolerance [5–7], but the underlying mechanisms remain unclear.

Interestingly, the protective efficacy of LEA proteins is not specific to the proteins of stress-tolerant organisms. For example, Goyal et al. [8] showed that AavLEA1, from the anhydrobiotic nematode, *Aphelenchus avenae*, provides anti-aggregation activity for pig heart citrate synthase (CS) and rabbit muscle lactate dehydrogenase under conditions of cold and desiccation stress. Chakrabortee et al. [9] demonstrated that AavLEA1 can prevent aggregation of human, as well as nematode, water-soluble proteomes. Furthermore, LEA protein protection is not limited to freeze and desiccation stresses, as AavLEA1 decreased the rate of aggregation of spontaneously aggregating

\*Present address: Proctor and Gamble, Temselaan 100, Grimbergen 1853, Belgium.

†These authors contributed equally to this work.

‡Present address: Department of Biochemistry, Tennis Court Road, Cambridge, U.K.

§Present address: School of Physical Sciences, University of Kent, Canterbury, Kent. CT2 7NZ.

Received: 23 November 2018

Revised: 18 March 2019

Accepted: 20 March 2019

Accepted Manuscript online:  
21 March 2019

Version of Record published:  
10 April 2019

proteins *in vitro* and *in vivo* in the absence of any stress [9,10]. The ability to prevent aggregation, which is not specific to the client protein or the stress, suggests that LEA proteins have a broad protein stabilisation function.

To gain a better understanding of the protective mechanism, we examine in detail a characteristic feature of LEA proteins: their ability to protect model folded proteins from aggregation through repeated cycles of freeze–thaw. We use CS as our model globular protein, and AavLEA1 [11] and ERD10 [12] as our model LEA proteins. Using a combination of pendant drop surface tension measurements and neutron reflection experiments, we find that CS, AavLEA1 and ERD10 are all surface active. However, the LEA proteins adsorb more rapidly to the interface and effectively out-compete CS, thereby reducing surface-induced CS aggregation. This novel LEA protein activity provides a general mechanism whereby members of this diverse family might provide non-specific protection to multiple folded proteins within cells during cold stress. It could also be relevant to other stresses where surface activity is a significant vector for protein denaturation.

## Materials and methods

### Proteins

Pig heart CS was purchased from Sigma–Aldrich as an ammonium sulfate suspension, and dialysed into water immediately prior to use.

Recombinant AavLEA1 was expressed in *Escherichia coli* BL21(DE3) cells, transformed with pET15b containing the AavLEA1 gene with an N-terminal thrombin cleavable hexa-histidine tag as described previously [13] with the modification that after induction with isopropyl- $\beta$ -D-thiogalactopyranoside (IPTG), cultures were grown at 23°C for a further 12 h. Cells were harvested by centrifugation, washed by resuspending in 10 mM Tris–HCl (pH 7.4) and 100 mM NaCl, recentrifuged and pellets stored at –20°C. Cells were later thawed and resuspended in IMAC A [10 mM sodium phosphate (pH 8.0), 0.5 M NaCl and 10 mM imidazole] with ‘complete’ EDTA-free protease inhibitor cocktail (Roche) before lysis by sonication. After sonication, the lysate was clarified by centrifugation at 18 000 rpm for 20 min, and the supernatant was heated to 100°C for 20 min before being recentrifuged at 13 000 rpm for 10 min. The supernatant was passed through a 0.22  $\mu$ m PVDF syringe filter and applied to a nickel chelation column (His-catch, Bioline or HisTrap FF Crude, GE Healthcare) pre-equilibrated with IMAC A. Bound proteins were eluted with IMAC B [10 mM sodium phosphate (pH 8.0), 0.5 M NaCl and 400 mM imidazole]. The histidine tag was removed by cleavage with thrombin, which was subsequently removed by passing over *p*-aminobenzamidine agarose (Sigma–Aldrich). Samples were extensively dialysed against water and concentrated using an Eppendorf 5301 vacuum concentrator in a cold room. AavLEA1 concentration was determined by absorbance at 280 nm using a molecular mass of 16 309.66 g/mol and a molar extinction coefficient of 8250 M<sup>–1</sup> cm<sup>–1</sup>.

Deuterated AavLEA1 (D-AavLEA1) was expressed and purified as described for AavLEA1 with the following modifications. After transformation, cells were acclimatised by plating sequentially onto LB agar plates containing 20%, 40%, 60% and 80% D<sub>2</sub>O. All growth steps were subsequently carried out in M9 minimal medium containing 100% D<sub>2</sub>O. After induction with IPTG, cultures were grown at 23°C for a further 48 h. Deuterium incorporation was determined by mass spectrometry (Protein & Nucleic Acid Chemistry Facility, Department of Biochemistry, University of Cambridge) and found to be ~90% for non-exchangeable protons.

The coding sequence for *Arabidopsis thaliana* ERD10 (European Nucleotide Archive EMBL-CDS: D17714.1) was PCR amplified from a plasmid [14] provided by David Macherel (University of Angers, France) and inserted into pHAT3.1 (based on pHAT3 [15] but with a modified polylinker in which the second BamHI site has been removed), which contains an N-terminal thrombin cleavable hexa-histidine tag, using BamHI and EcoRI. Recombinant ERD10 was expressed and purified essentially as described for AavLEA1. However, after removal of the histidine tag, ERD10 was dialysed into 20 mM Tris (pH 8.0) before further purifying on a 6 ml Resource Q column (GE Healthcare) using a linear salt gradient from 0 to 1 M NaCl in Tris–HCl (pH 8.0) over 100 ml. The purified protein was then dialysed extensively against H<sub>2</sub>O, and the concentration was determined by absorbance at 280 nm using a molecular mass of 29 691.90 g/mol and a molar extinction coefficient of 2560 M<sup>–1</sup> cm<sup>–1</sup>.

### *In vitro* protein freeze–stress aggregation assay

Samples of 200  $\mu$ l were loaded into a 96-well plate, submerged in liquid nitrogen for 10 min, and thawed at 20°C. After each freeze–thaw cycle, the extent of aggregation was determined by measuring the apparent

absorbance at 340 nm using a Wallac EnVision 2104 Multilabel plate reader. To examine the effect of degassing, samples were degassed for 10 min in an Eppendorf 5301 vacuum concentrator in advance of each freeze–thaw cycle. Different freezing rates were achieved by substituting the liquid nitrogen freezing step with placing the samples in a  $-20^{\circ}\text{C}$  freezer or  $-80^{\circ}\text{C}$  freezer for 8 h.

### Cavitation–stress aggregation assay

Cavitation was induced in 400  $\mu\text{l}$  samples using an ultrasonic probe, SLPe Digital Sonifier (Branson<sup>TM</sup>) in a cold room. Cycles were 30 min at 10% amplitude. After each cycle, aggregation was measured by apparent absorbance at 340 nm using a Wallac EnVision 2104 Multilabel plate reader.

### Foaming performance

The Bartsch cylinder shake test [16] was used to evaluate the foaming collapse profiles of protein solutions. Closed 10 ml cylinders with 1 ml of each protein solution were vigorously shaken by hand 10 times, once per second, over 10 s. The foam volume was measured every minute over 6.5 h. The foamability of a solution was characterised by the foam volume immediately after shaking, and the foam stability was characterised by the foam volume remaining at each time point.

### Surface tension measurements

Surface tension data were obtained using a DSA 100 Drop Shape Analysis System (Krüss GmbH, Germany). Approximately 25  $\mu\text{l}$  drops of protein in water at various concentrations were suspended from a 1.830 mm diameter syringe needle. Photos were taken at an average speed of 3 fps and the drop shape was monitored over 15 min. The shape factor was iterated from the photos of the drops by the DSA1 software. Times shown in the data denote the time since the first measurement. It takes  $\sim 8$  s, from the first depression of the syringe plunger (liquid exiting the needle), for the drop to be formed and to stabilise. Therefore, changes during the first 8 s are not measured using this system.

### Small-angle neutron scattering measurements

Small-angle neutron scattering (SANS) experiments were performed with the Sans2D time-of-flight instrument at ISIS located at the Rutherford Appleton Laboratory in Oxfordshire, U.K. The detector length was 4 m and the incident wavelength of the neutron beam was 1.75–16.5 Å. This gave a  $Q$  range of 0.005–0.6 Å<sup>-1</sup>. QS quartz banjo cells with an optical path of 1 or 2 mm were used. Temperature control was carried out using 5 kW circulating fluid baths and set to 7°C. Typically, data were collected for 30 min and then corrected and normalised to an absolute scale by background subtraction. Data were analysed using the SasView-2.2.1 program ([www.sasview.org](http://www.sasview.org)).

The freeze–thaw experiments were performed using 0.25 or 0.5 ml samples contained in 1.5 ml Eppendorf tubes. The samples were frozen for 5 min in liquid nitrogen and thawed in an ambient temperature water bath for 7 min. Three models were used to fit the SANS data. For CS, an ellipsoid model describing an ellipsoidal particle with a uniform scattering length density and without inter-particle interactions was used. For hydrogenated AavLEA1 (H-AavLEA1), a polydisperse Gaussian-coil model was used. This describes polymer chains with a well-defined molecular mass distribution. For D-AavLEA1, a correlation length model was used. This is an empirical model which describes the representative length scale for the protein chains.

### Neutron reflection at the air–water interface

Neutron reflection experiments were undertaken on the Fluid Interfaces Grazing Angles Reflectometer (FIGARO) time-of-flight reflectometer at the Institut Laue-Langevin (ILL), Grenoble, France. The protein solutions were loaded onto low-volume Delrin troughs with a positive meniscus to ensure that the trough itself does not obstruct the incoming or reflected neutron beams. The troughs were mounted onto an active antivibration table and automatically aligned using a high precision optical sensor. The temperature was set at 20°C.

Measurements were conducted at one incident angle and at a wavelength range of 2 Å <  $\lambda$  < 30 Å, which covers a  $Q$  range from 0.008 to 0.4 Å<sup>-1</sup>. All noted surface ages are measured from the time of sample spreading. For single protein samples and for the CS + AavLEA1 sample measured at 2 h, the measurement time ranged from 45 min to 1.5 h, depending on the contrast. For younger surface ages, the data were collected for 30 s.

The RASCAL standard discrete layer approaches customarily used to fit neutron reflection data were insufficient to accurately describe our system. Therefore, a new custom layer model approach was used. This new, more flexible model contains ‘thickness’ as a fitted variable and assumes that there is no protein at either the top (i.e. the air boundary) or below the surface protein layer (the bulk). The fitting was done on all contrasts simultaneously. For each data set, 11 parameters were designated: the thickness of the entire surface layer measured and, for each protein, the protein concentration at five equally spaced points within the surface layer (10 parameters in total). Five points allowed for sufficient flexibility in the model while keeping the number of fitted variables low. All parameters were allowed to fit freely between 0 and 100%. For each protein concentration point, the SLD was calculated by simply summing the SLD contributions from each protein (protein concentration multiplied by the protein SLD) with the SLD contribution of the bulk SLD. The in-between protein concentrations were constructed using PCHIP interpolation and the entire protein concentration curve was then fit with the data and the Chi-squared measured. The fits were performed using alternating Simplex and Covariance Matrix Adaption Evolution Strategy procedures until the minimum Chi-squared was reached. For each dataset, the fitting was repeated six times with different initial points and the result with lowest Chi-squared was selected.

### Far-UV circular dichroism spectroscopy

Circular dichroism (CD) spectra of H-AavLEA1 and D-AavLEA1 at a concentration of 8–12.3  $\mu\text{M}$  in  $\text{H}_2\text{O}$ , 42%  $\text{D}_2\text{O}$  and  $\text{D}_2\text{O}$  were recorded over the range 190–250 nm using an AVIV 410 spectrometer. Spectra were recorded at 25°C in a 1 mm path-length cuvette with a data pitch of 1 nm, an averaging time of 2 s and baseline corrected against the appropriate solvent before applying smoothing. Measured ellipticity values were converted to mean residue ellipticities (MREs) with units  $\text{deg cm}^2 \text{dmol}^{-1}$  to normalise for differences in concentration. Secondary structure analyses were carried out using the DichroWeb online server [17] with the CONTIN-LL algorithm [18,19] and reference dataset seven [20].

## Results

### AavLEA1 suppresses aggregation of CS during freeze–thaw stress

CS is prone to aggregation upon freeze–thaw and has previously been used to examine the protective role of LEA proteins [7–9]. We first confirmed that AavLEA1 could suppress CS aggregation during freeze stress in pure water, without the influence of buffer components [21]. When subjected to successive rounds of rapid freezing in liquid nitrogen followed by thawing at 20°C, CS samples showed an increase in turbidity (measured by apparent absorbance at 340 nm;  $A_{340}$ ), which is indicative of light scattering by protein aggregates in suspension (Figure 1a). In contrast, when both CS and AavLEA1 were present in solution at a 1:1 CS:AavLEA1 mass ratio ( $\sim 1:5$  CS:AavLEA1 molar ratio), samples exhibited consistently low turbidity values, similar to those prior to application of the stress. AavLEA1 alone does not aggregate under these conditions (data not shown). These results are consistent with those reported by Goyal et al. [8].

### No LEA protein–client interactions in the bulk either before or after freezing

It has been proposed that the protective effect of LEA proteins involves little, or at most only transient, interaction with client proteins, and they have therefore been termed ‘molecular shields’ [7]. However, any such interactions are usually assayed in the absence of stress, and a detailed understanding of any LEA–client interactions or structural changes in either partner that occur upon freeze–thaw is lacking.

To examine this we chose to use SANS. Because we were able to produce both hydrogenated and D-AavLEA1 recombinantly in *E. coli*, we were able to use contrast matching to look at the individual components in the mixture. The contrast of the solvent can be changed by altering the  $\text{H}_2\text{O}/\text{D}_2\text{O}$  ratio allowing the selective ‘matching out’ of D-AavLEA1 with 100%  $\text{D}_2\text{O}$  and hydrogenated CS with 42%  $\text{D}_2\text{O}$ .

Before looking at the CS and AavLEA1 proteins together, it was important to confirm that deuteration of the protein did not adversely affect function, since the strength of hydrogen bonds and the dissociation constants of ionisable groups in the protein will be different depending on whether H or D is present. Therefore, we compared the ability of H-AavLEA1 and D-AavLEA1 proteins to protect CS from freeze–thaw-induced aggregation in both  $\text{H}_2\text{O}$  and  $\text{D}_2\text{O}$ . Furthermore, any effects on secondary structure were assessed by CD spectroscopy. As shown in Figure 1b,c, both H-AavLEA1 and D-AavLEA1 provided similar levels of freeze–thaw protection in both solvents, and the CD spectra of both proteins (Figure 1d,e) are typical of IDPs, with a large

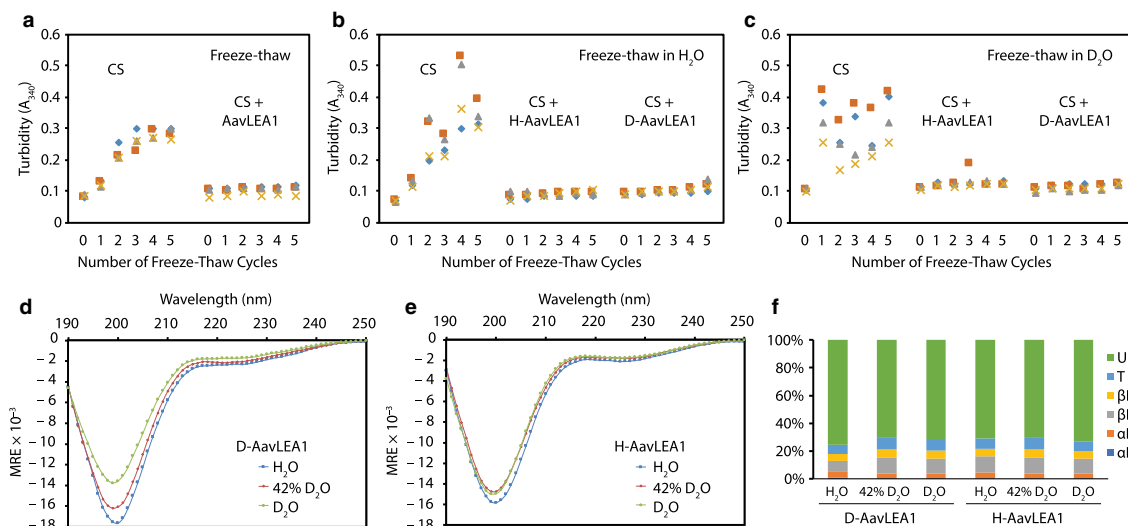


**Figure 1. Cryoprotective and structural properties of hydrogenated and D-AavLEA1.**

(a) Aggregation of CS in the absence and presence of AavLEA1 before and after the indicated number of freeze–thaw cycles was monitored by turbidity measurements at 340 nm. Freeze–thaw assays comparing the protective efficacy of H- and D-AavLEA1 for CS in (b) H<sub>2</sub>O and (c) D<sub>2</sub>O. Concentrations of CS and H-/D-AavLEA1 were 0.25 mg/ml. Individual data points for each replicate are shown. Far-UV CD spectra of (d) D-AavLEA1 and (e) H-AavLEA1 in H<sub>2</sub>O, 42% D<sub>2</sub>O and D<sub>2</sub>O. Data are displayed as MRE to normalise for differences in concentration. (f) Predicted secondary structure content of H-AavLEA1 and D-AavLEA1 in H<sub>2</sub>O, 42% D<sub>2</sub>O and D<sub>2</sub>O, assigned according to the six classification system devised by Woody and co-workers [22]: αR, alpha helix (regular); αD, alpha helix (distorted); βR, beta sheet (regular); βD, beta sheet (distorted); T, turn; U, unordered.

‘random-coil’ minimum and evidence of a small amount of secondary structure. Although there are some differences between the spectra, especially for D-AavLEA1 in the different solvents, the predicted secondary structure content in all cases was similar and indicated that the proteins are predominantly (>70%) disordered (Figure 1f).

The SANS pattern from CS dispersed in D<sub>2</sub>O is shown in Figure 2a. The data fit well to an ellipsoid model of CS with the two radii being  $18.0 \pm 0.2$  and  $45.1 \pm 0.2$  Å. The scattering patterns and fits for the AavLEA1 proteins are shown in Figure 2b,c. It is clear the scattering patterns of the H-AavLEA1 and D-AavLEA1 proteins look different. Intriguingly, while the H-AavLEA1 protein scattering fits to a Gaussian coil with a radius of gyration of  $\sim 33$  Å as one might expect for a disordered protein, the D-AavLEA1 protein does not and was best fit by a correlation length model of size 13 Å. This indicates that while both the H- and D-forms of the protein are similar in terms of secondary structure content (Figure 1f), the overall properties of the ensemble, to which SANS is more sensitive, are different. Alternatively, the high protein concentrations required for the SANS experiments induced weak aggregation in D-AavLEA1 and resulted in a different scattering pattern. In the preparations of the samples, it was noticed that the solubility of D-AavLEA1 was lower than that of H-AavLEA1. A common assumption in neutron scattering is that deuteration does not affect a molecule’s structure, but this is clearly not the case here; perhaps, IDPs are more prone to the subtle differences induced by replacing H with D [23–25]. However, any structural changes did not appear to significantly affect function, with the H- and D-AavLEA1 proteins both protecting CS from freeze–thaw-induced aggregation in both H<sub>2</sub>O and D<sub>2</sub>O (Figure 1b,c).

Consequently, we proceeded to examine the individual proteins and the mixtures of CS with D-AavLEA1 both before and after freeze–thaw stress. Before freezing, the scattering profiles of the two proteins in the mixture corresponded to those of the individual proteins, consistent with previous data showing that AavLEA1 does not stably associate with client proteins [7]. Samples were then subjected to one or three rounds of freeze–thaw and scattering profiles recorded. Samples containing CS alone were seen to visibly aggregate following freeze–thaw. Consistent with this, SANS curves (Figure 2d) showed an upturn at low Q which was progressive

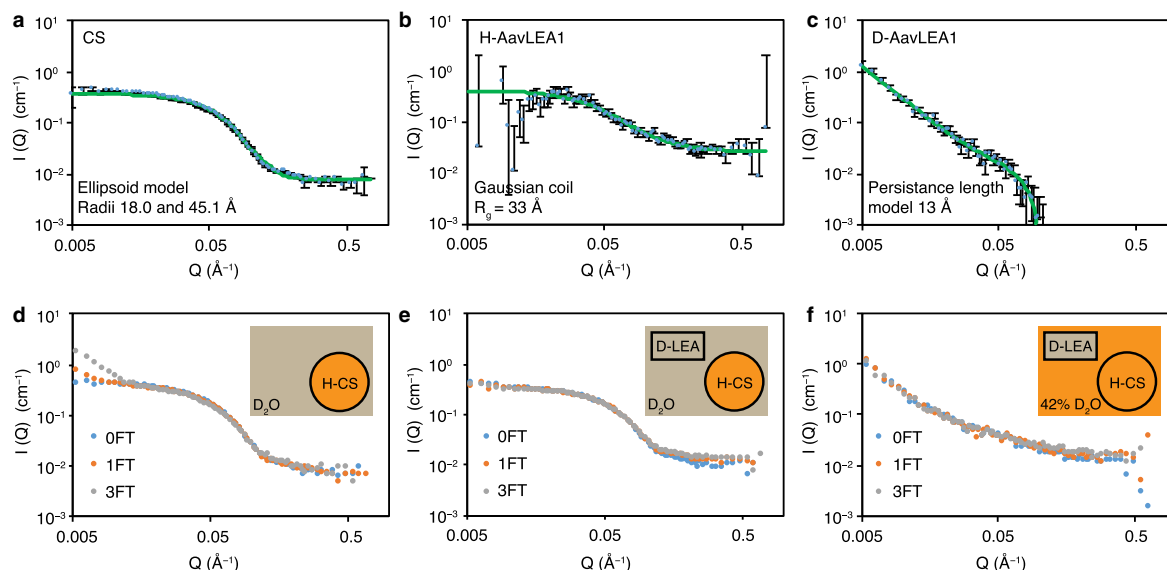


**Figure 2. SANS analysis of CS, AavLEA1 and the mixture before and after freeze–thaw.**

SANS curves recorded for (a) 2.5 mg/ml H-CS in D<sub>2</sub>O, (b) 2.5 mg/ml H-AavLEA1 in D<sub>2</sub>O (N.B. low Q points were removed because of over subtraction of the background) and (c) 2.5 mg/ml D-AavLEA1 in 42% D<sub>2</sub>O. The error bars in the SANS data correspond to the standard deviation in the neutron flux intensity. Best fits obtained for the data using SasView-2.2.1 are shown. SANS curves for (d) 2.5 mg/ml H-CS in D<sub>2</sub>O, (e) 2.5 mg/ml H-CS + 2.5 mg/ml D-AavLEA1 (D-AavLEA1 is contrast matched out by solvent), and (f) 2.5 mg/ml H-CS + 2.5 mg/ml D-AavLEA1 in 42% D<sub>2</sub>O (H-CS is contrast matched out by solvent), after zero, one cycle and three cycles of freeze–thaw.

with successive rounds of freeze–thaw, indicative of aggregation. Interestingly, there were no major changes in the high Q region of the scattering curve, suggesting that any conformational changes in the CS dimer are only minor. In the presence of AavLEA1, this upturn was not observed (Figure 2e), and the curves for different numbers of freeze–thaw cycles overlay. Finally, the profiles for D-AavLEA1 in the presence of CS before and after freeze–thaw look identical (Figure 2f). Taken together, these data show that there is no apparent change in protein structure or long-range ordering of the system, even after three cycles of freeze–thaw. It is important to note that we have not measured the system in the frozen state, so we are unable to rule out the involvement of transient interactions that occur during freezing and thawing, our data indicate that any interactions do not endure beyond the imposition of stress.

## Air–water interfaces are involved in CS aggregation

During the freeze–thaw process, a large number of air bubbles were observed. Protein denaturation and/or aggregation at interfaces is a well-known phenomenon [26–29]. Therefore, we investigated the effect of bubble formation on CS stability using several complementary methods.

First, the concentration of dissolved gasses was reduced by vacuum degassing samples prior to each freezing cycle. The degassed CS samples, even without the addition of AavLEA1, showed reduced turbidity (Figure 3a), confirming that dissolved gasses were, at least in part, responsible for CS aggregation during freeze stress. However, degassing samples did not reduce CS aggregation to the levels observed in the presence of AavLEA1. This difference might be due to incomplete degassing or to the effect of other interfaces or stressors.

Another factor that influences bubble formation is freezing rate. Dissolved gasses are excluded from ice crystals during the freezing process. Rapid freezing traps the bubbles, which remain in the sample until thawing occurs. In contrast, at low freezing rates, these gas bubbles have time to coalesce, reducing the surface area, and are pushed in front of the ice surface, allowing them to escape as the sample freezes [30]. Freezing rate also influences the surface area of the ice–water interface produced. Hence, slower freezing is less detrimental to protein stability [31,32]. Consistent with this, CS samples flash frozen in liquid nitrogen gave much higher

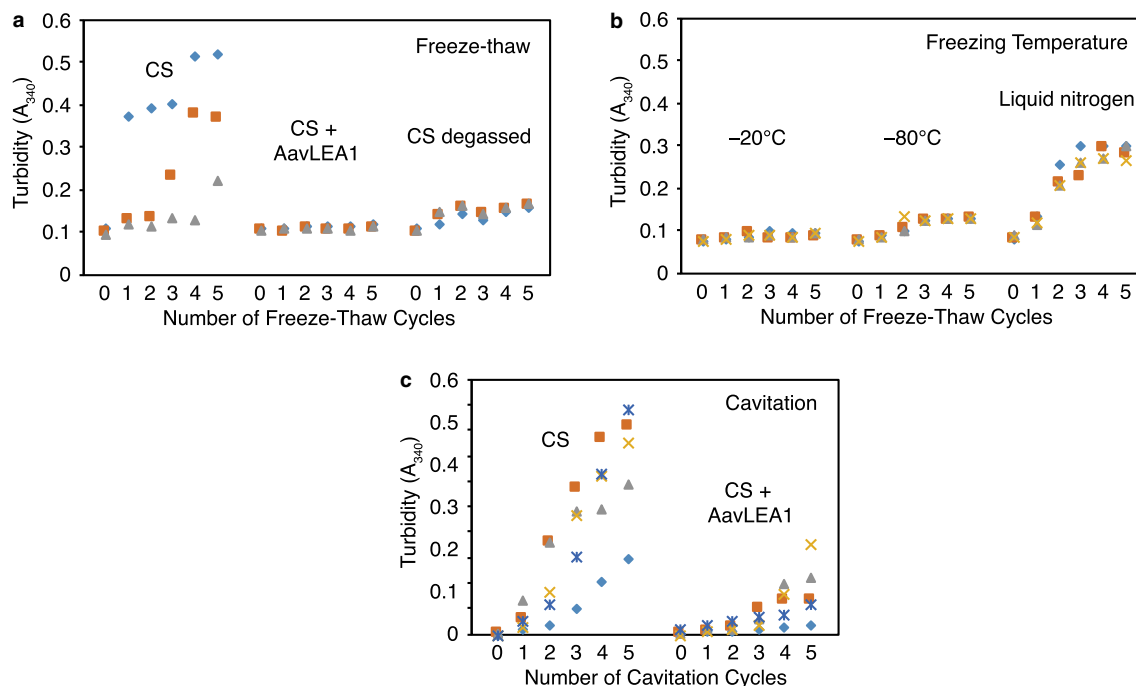


**Figure 3. LEA proteins prevent CS aggregation caused by exposure to gas–liquid interfaces.**

Turbidity measured at 340 nm of solutions containing (a) CS, CS + AavLEA1, and CS (degassed) after multiple freeze–thaw cycles; (b) CS after multiple cycles of freeze–thaw at  $-20^{\circ}\text{C}$ ,  $-80^{\circ}\text{C}$  and in liquid nitrogen; (c) CS in the absence and presence of AavLEA1 after multiple cycles of sonication. Concentrations of CS and AavLEA1 were 0.25 mg/ml. Individual data points for each replicate are shown.

turbidity readings than identical samples frozen at  $-80^{\circ}\text{C}$  or  $-20^{\circ}\text{C}$ , with the latter showing very little evidence of aggregation (Figure 3b).

Finally, we investigated the effect on CS aggregation of bubble formation in the absence of freeze–thaw stress; this was achieved by sonication, which induces cavitation (the formation and collapse of tiny bubbles within a liquid due to rapid and intense pressure changes) in the sample (Figure 3c). Ultrasonic treatment is known to cause protein condensation at the surface of gas bubbles, forming aggregates [33]. Samples of CS in the absence or presence of AavLEA1 were subjected to multiple rounds of sonication using an ultrasonic probe and aggregation was monitored as before. CS alone readily aggregated; turbidity readings were much higher than observed during freeze–thaw assays, indicating that either more of the protein had aggregated or that larger aggregates had formed. Interestingly, samples containing CS and AavLEA1 showed much lower levels of aggregation after cavitation, with significant measurable aggregation not seen until after three rounds of cavitation, suggesting that the mechanism of protection by AavLEA1 involves gas–liquid interfaces. In contrast with the freeze–thaw experiments, protection was incomplete. This may be due to the heating that occurs during sonication, as AavLEA1 alone cannot prevent thermal aggregation of CS [8].

Gas–liquid interfaces are characteristic of both flash freezing and sonication; therefore, we hypothesised that the mechanism of protection by LEA proteins during freeze–thaw may be related to the propensity of air–water interfaces to promote protein aggregation.

## LEA proteins adsorb to air–water interfaces in preference to CS

The foamability and foam stability of a protein solution are dependent on adsorption rates and the structure of proteins at the interface. Good foamability correlates with a protein's affinity for the air–water interface, which results in increased adsorption and a more rapid decrease in dynamic surface tension.

The foaming properties of CS and AavLEA1 were found to be very different. Foamability of CS samples was very low; when shaken, CS samples formed a few bubbles which immediately collapsed, and the foam height

was considered negligible. In contrast, AavLEA1 solutions formed foams that were stable for several hours. This difference in foamability indicates that AavLEA1 adsorbs to the air–water interface more readily than CS. Figure 4a shows the foam collapse profiles of CS, AavLEA1 and a mixture of CS and AavLEA1. While CS showed negligible foaming, both AavLEA1 and the mixture of the two proteins showed similar foam collapse profiles, indicating that the foaming properties of the mixture are dominated by the disordered LEA protein.

To examine the adsorption at the air–water interface over time, dynamic surface tension profiles for CS, AavLEA1 and mixtures of the two proteins were measured using the pendant drop method (Figure 4b). Briefly, the protein concentration at a newly created interface is zero; therefore, the surface tension when a surface is created is expected to be that of pure water. Surface tension then decreases as protein adsorbs to the interface, until the interface is saturated. The profile for AavLEA1 resembles that of a typical surfactant; surface tension rapidly decreased until ~60 s and then plateaued, indicating that equilibrium had been reached. Interpretation of the CS data is more complicated. There is an initial decrease in surface tension over the first 150–200 s, and then a second (slower), decrease that does not reach completion even after 900 s. Presumably, the first process represents adsorption of native CS to the interface, and the second slower process represents a structural rearrangement or denaturation of the globular protein at the interface, because exposure of hydrophobic residues would lower the surface energy.

The initial decrease in dynamic surface tension for AavLEA1 was more rapid than for CS, indicating that AavLEA1 became established at the interface more quickly. This is consistent with our foaming results.

Adding increasing concentrations of AavLEA1 to CS resulted in the dynamic surface tension profiles of the mixtures converging with that of AavLEA1 alone. At low AavLEA1 concentrations, the mixture still exhibited an initial ‘fast’ decrease in surface tension, similar to AavLEA1, but then a second much slower decrease, similar to CS, indicating that some CS reaches the interface. When sufficient AavLEA1 was present, the profiles

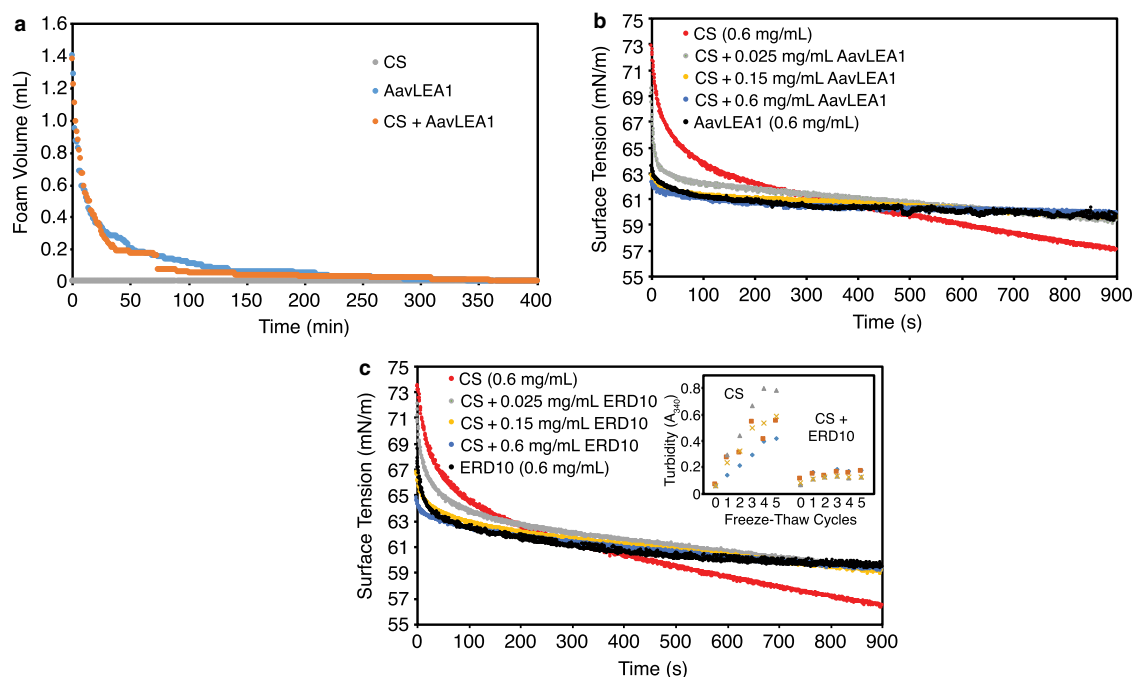


**Figure 4. Characterising the surface activity of CS, AavLEA1 and ERD10.**

(a) Foam collapse profiles of CS, AavLEA1 and CS + AavLEA1 solutions. The concentration of CS and AavLEA1 was 0.25 mg/ml. Closed 10 ml cylinders with 1 ml of each protein solution were vigorously shaken by hand 10 times, once per second, over 10 s and the foam volume was measured every minute over 6.5 h. Dynamic surface tension profiles of CS (0.6 mg/ml) in the absence or presence of increasing concentrations of (b) AavLEA1 and (c) ERD10 (as indicated). The surface tension of each solution was monitored over 15 min using the pendant drop method. Time = 0 s denotes the start of measurement at ~8 s after the start of drop formation. The inlay to (c) shows turbidity measurements for CS and CS in the presence of ERD10 before and after the indicated number of freeze–thaw cycles.



looked almost identical with that of AavLEA1 alone, suggesting that CS did not populate the surface significantly. These dynamic surface tension profiles are similar to those observed in protein/surfactant mixtures where the surfactant outcompetes the protein to dominate the interface [34,35]. Taken together, the surface tension data suggest that AavLEA1 adsorbs to the surface more quickly than CS, and in the presence of sufficient AavLEA1, CS competes poorly for access to the surface.

The foaming and surface tension data, taken together, are consistent with the observation that proteins with more ‘flexible’ structures tend to bring about more rapid changes in dynamic surface tension and form more stable foams than those with rigid structures [36–38].

To demonstrate that the competitive adsorption effect was not limited to AavLEA1, similar freeze–thaw and surface tension experiments were performed with another LEA protein, ERD10, from *A. thaliana*. Despite significantly different characteristic amino acid signatures, and being from a different LEA protein group (Supplementary Figure S1), freeze–thaw experiments showed that ERD10 also provided good protection against CS aggregation (Figure 4c, inset). Dynamic surface tension experiments showed that like AavLEA1, ERD10 also adsorbed at the air–water interface preferentially to CS (Figure 4c).

## Neutron reflection analysis of the surface layer conformations of disordered LEA and globular CS proteins at air–water interfaces

The dynamic surface tension data provided evidence that AavLEA1 preferentially adsorbs to the air–water interface; however, the method was unable to easily differentiate the contributions of each protein in the mixtures. Therefore, to provide a fuller picture of the system, neutron reflection was used. D-AavLEA1 protein was produced recombinantly as described in the Materials and Methods section. This allowed the different components in the protein mixture to be individually examined. In 100% D<sub>2</sub>O, only contributions from the air–water interface and hydrogenated proteins are detected (deuterated proteins are ‘matched out’). In 42% D<sub>2</sub>O, only contributions from deuterated proteins and the substrate are recorded (hydrogenated proteins are ‘matched out’). Finally, using ‘air contrast matched water’ (8% D<sub>2</sub>O), contributions from the substrate (water) can be ‘matched out’. By simultaneously fitting the data from multiple different contrasts, density profiles for each protein can be calculated.

Thorough attempts were made to fit the neutron reflection data using the standard discrete layer fitting approach in RASCAL. However, the inability to provide a good fit to the data indicated that the proteins were not present in distinct layers of single proteins. Therefore, a new, more flexible, custom layer model was written to fit the reflectivity profiles to provide protein concentration versus depth profiles. The reflectivity profiles and fitted curves are shown in the insert to each protein density curve.

First, the two proteins were examined individually. The reflectivity profiles of CS in water after equilibrating for 2 h, in three different water contrasts, are shown in the inset to Figure 5a. The fit to the data is shown as solid lines, resulting in the protein density profile shown in Figure 5a. This shows a multi-layer configuration with a total thickness of ~8 nm. The layer closest to the air–water interface was estimated to be ~2.5 nm thick, which is too small to be native CS, suggesting that the protein at the surface has undergone a structural rearrangement. This is consistent with our surface tension observations, where we hypothesise that after initial adsorption to the surface, CS then undergoes a slower conformational rearrangement. There is additional CS just below this denatured surface layer extending a further 5 nm, which may comprise of one or two additional layers where molecules are more diffuse and less well organised.

The inset of Figure 5b shows the reflectivity profiles for both H-AavLEA1 and D-AavLEA1 proteins in three different water contrasts after 2 h. These profiles are simultaneously fit to provide the protein density profile shown in Figure 5b. In contrast with CS, AavLEA1 formed a concentrated layer ~2 nm thick at the interface, with a more diffuse zone extending to a depth of 5 nm below the interface. It is difficult to draw detailed conclusions about the structure of AavLEA1 at the interface because the protein is intrinsically disordered; however, the thickness of the dense layer closest to the surface is smaller than the size of a single AavLEA1 molecule, determined by SANS as 3.3 nm. This suggests that the AavLEA1 protein either spreads out or takes a conformation at the interface which is more compact than in the bulk. The simultaneous fit of H- and D-AavLEA1 indicates that the proteins take up similar structures at the air–water interface, despite the finding in Figure 2b,c, showing a difference in bulk structure. Hence, our belief is that the difference only occurs in the bulk at elevated concentrations. Previous Fourier transform-infrared spectroscopy studies have shown that AavLEA1, although natively unfolded in bulk solution, could be induced into helical formations by drying [13],

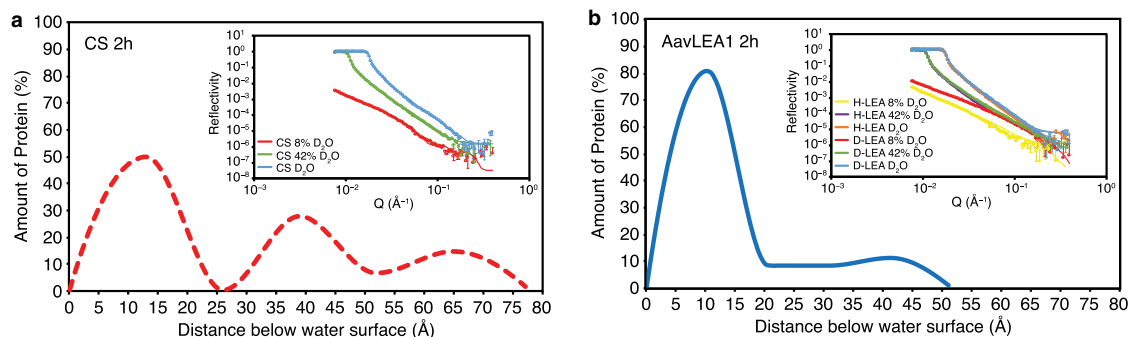


**Figure 5. Using neutron reflectivity to study CS and AavLEA1 at the air–water interface.**

Protein concentration profiles of (a) 0.6 mg/ml CS and (b) 0.6 mg/ml AavLEA1 at the air–water interface. Neutron reflectivity curves recorded at several contrasts (see inlays) were simultaneously fit using a new custom layer approach (see Materials and Methods) to give the resulting profiles. In the insert caption, D-AavLEA1 is denoted as D-LEA and H-AavLEA1 is denoted as H-LEA. Chi-squared values of the resulting fits may be found in Supplementary Table S1.

consistent with secondary structure predictions and computer modelling of AavLEA1 and other similar LEA protein structures [13,39,40]. Similar to drying, the air–water interface might also decrease protein hydration and exert a thermodynamic pressure for AavLEA1 to adopt a more compact structure. These neutron reflection results confirm that both AavLEA1 and CS have the propensity to adsorb to the air–water interface, which is consistent with the surface tension measurements.

Next, competitive adsorption experiments using mixtures of CS and AavLEA1 were conducted at a single detector position over 30 s intervals. This allowed data to be collected at short time points showing how the protein density profiles evolve with time (Figure 6). All contrasts were fit simultaneously and, in all profiles, the surface was clearly dominated by AavLEA1. Consistent with the dynamic surface tension measurements, a significant amount of AavLEA1 had adsorbed to the surface after only 30 s, forming two distinct layers (Figure 6a). No contribution from CS was apparent until the 30-min time point (Figure 6d), when a small amount of CS was detected ~5 nm below the interface. By 60 min, some CS started to appear in a bilayer conformation (Figure 6e). By 2 h, a measurable bilayer of CS was formed at the interface (Figure 6f); however, the layer of protein closest to the interface was still predominantly composed of AavLEA1. These results provide further evidence that AavLEA1 outcompetes CS for access to the interface over short time frames and thus reduces surface-induced aggregation of CS.

## Discussion

Proteins have been shown to lose biological activity after exposure to interfaces [41,42]. In solution, globular proteins are marginally stable [43] and their adsorption to interfaces causes aggregation [26,27]. During the freeze–thaw process, many new interfaces are created, most notably those associated with air bubbles, due to the precipitation of dissolved gasses during freezing, and ice crystals. Proteins readily adsorb to these interfaces, which are believed to be denaturation sites for folded proteins [31,44–47]. Here, we investigated how two IDPs associated with tolerance to water stress, the LEA proteins AavLEA1 and ERD10 protect a model globular protein, CS, from freeze–thaw-induced protein aggregation. In comparison with globular proteins, LEA proteins are usually lower in molecular mass and far more ‘flexible’ in structure. Although they contain a high proportion of charged and polar amino acids, LEA proteins also contain hydrophobic residues, and both types of residues are potentially available for interaction with interfaces. Our results provide evidence that AavLEA1 outcompetes CS at an air–water interface, and that this ability may allow AavLEA1 to protect CS from surface-induced denaturation. These findings have led us to propose preferential adsorption to interfaces as an additional, novel mechanism by which LEA proteins can stabilise folded proteins during stress. We hypothesise that this activity, during freeze–thaw, effectively restricts a protein such as CS to the bulk liquid, thus protecting it from denaturation at the interface. This new mechanism is consistent with studies showing that the aggregation of proteins exposed to air–water interfaces can be reduced by the addition of surfactants [28,31,46]. LEA proteins could fulfil a similar role to that of the surfactants in these studies, but with the advantage of better

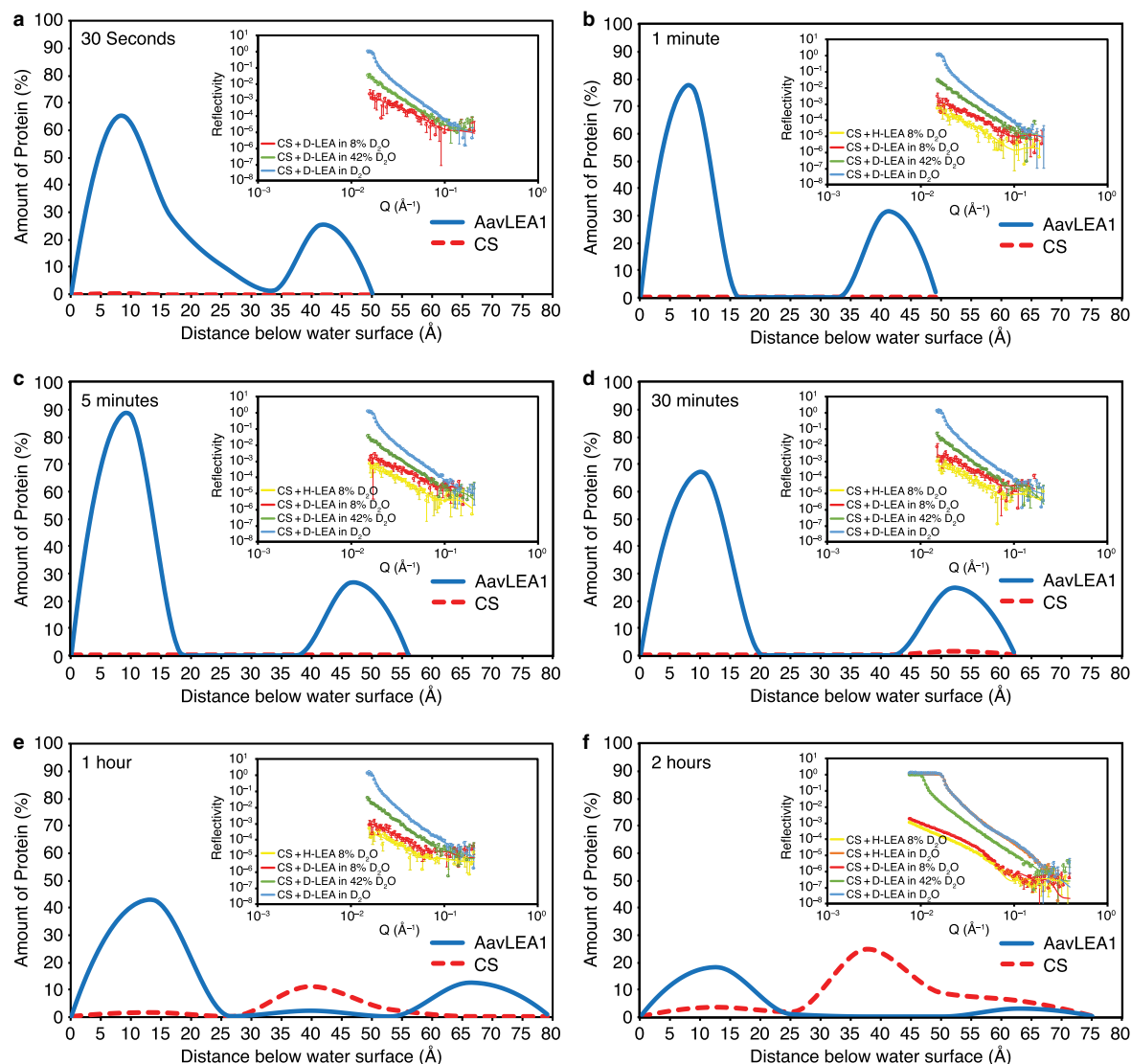


**Figure 6. Preferential adsorption of AavLEA1 to the air–water interface followed by neutron reflectivity.**

Protein concentration profiles of a mixture of 0.6 mg/ml CS and 0.6 mg/ml AavLEA1 obtained from fitting neutron reflection data recorded at the following time points, (a) 30 s, (b) 1 min, (c) 5 min, (d) 30 min, (e) 1 h and (f) 2 h. Inlays show the reflectivity profiles recorded at the indicated contrasts that were simultaneously fit to generate the concentration profiles. In the insert caption, D-AavLEA1 is denoted as D-LEA and H-AavLEA1 is denoted as H-LEA. Chi-squared values of the resulting fits may be found in Supplementary Table S1.

biological compatibility. In this study, we have mainly focused on the effect of air–water interfaces; however, our degassing experiments suggest that additional factors contribute to CS denaturation upon freeze–thawing. There is a growing body of evidence supporting the idea that loss of folded protein integrity during the freezing process is at least partially due to denaturation at the ice–water interface [31,44–47]. We speculate that a similar preferential adsorption mechanism might also occur at this interface, and this is the subject of ongoing work.

The proposal that LEA proteins adsorb to interfaces as a method of globular protein protection aligns with the evidence that protection is non-specific with respect to the client protein, the LEA protein, and the type of stress. LEA proteins protect a variety of different folded proteins and even entire proteomes from desiccation-induced aggregation [8,9]. In addition, there are many LEA proteins, with varying amino acid motifs, which have been shown to protect against freeze stress [48–50]. The group 2 (ERD10) and group 3

(AavLEA1) LEA proteins used in this study were both shown to provide good protection for the same client protein, even though their sequences, molecular mass and signature motifs differ significantly (Supplementary Figure S1). An interfacial adsorption mechanism would only require the LEA protein to out-compete the client protein for the interface. As unstructured, low molecular mass macromolecules, these characteristics would be expected for any LEA protein with the correct hydrophilic–hydrophobic balance.

The proposed preferential adsorption model for LEA proteins provides a general mechanism that explains how LEA proteins are able to protect client proteins from aggregation under a variety of stresses. However, even in the absence of any stress, interfaces can be damaging to proteins. LEA proteins have been shown to decrease the rate of aggregation of spontaneously aggregating polyQ proteins *in vitro* and *in vivo* [9,10]. Recent observations suggest that polyQ proteins may have the propensity to aggregate at gas bubble interfaces [51]. Therefore, interfacial adsorption of LEA proteins may also play a significant role in preventing polyQ aggregation. Since interfacial competition by LEA proteins is a general aggregation protection mechanism (i.e. one that does not require specific interaction with a client protein), the results from this work may be applicable to other protein systems where interfaces are found to nucleate protein aggregation, e.g. amyloids characteristic of Alzheimer's disease [52].

The tendency of LEA proteins to migrate to air–water interfaces is reminiscent of models that explain their protection of lipid bilayers under water-stress conditions. Thus, various LEA proteins are thought, during cold stress or dehydration, to fold into amphipathic helices that become embedded laterally in the surface of the membrane [53,54]. In this 'snorkeling' model [55,56], the hydrophobic surface of the helix penetrates below the headgroup region of the bilayer to interact with the fatty acid side chains of the phospholipids [54,57]. The hydrophilic face of the LEA protein remains in contact with the headgroups and any associated water molecules. The air–water interface in gas bubbles might also provoke folding of LEA proteins into helices such that the hydrophobic face projects into air, while the hydrophilic surface remains in the liquid phase.

The neutron reflectivity and surface tension data suggest that both CS and AavLEA1 rearrange upon contact with the air–water interface. CS adsorption sees a two-stage reduction in surface tension which we ascribe to adsorption and then a subsequent slower rearrangement. This is consistent with the neutron reflectivity data, which shows a surface layer smaller than the native bulk CS. Adsorption of AavLEA1 has only a single relaxation time in the surface tension measurements, indicating that any rearrangement does not correlate with a surface tension reduction. The neutron reflection data show a surface layer which is more compact than the native protein, again indicating a change in structure. We note also that the IDP can be easily redispersed and does not denature, showing that any surface-induced structure is transitory. Our comments about interface-induced restructuring are indirect inferences from the surface tension and reflectivity. It would be desirable to obtain a direct measure of structure at the interface and this is the subject of future work.

The preferential adsorption of LEA proteins to the air–water interface is also, to some extent, comparable with the Vroman effect, which describes the competitive adsorption of proteins to a solid surface [58]. In a mixture of proteins, smaller or more highly concentrated proteins are the first to arrive at and adsorb to a solid–liquid interface, and these are later displaced by proteins of higher molecular mass [59]. Similarly, for mixtures of CS and LEA protein, our neutron reflection data suggest that although initially AavLEA1 dominates the air–water interface, CS can begin to compete for the surface over long time periods. Whether such an exchange would occur at an appreciable rate at low temperatures is perhaps unlikely, particularly where cells freeze.

IDPs are known to protect globular proteins through both freeze–thaw and desiccation stresses. In this work, we have only examined the freeze–thaw-induced aggregation although we note that the presence of air–water interfaces is common to the stresses that IDPs are known to offer protection from.

Taken together, our results indicate that AavLEA1 effectively competes with CS for access to the interface over short time-scales, providing protection against surface-induced aggregation in freeze–thaw assays. However, the data from longer time points indicate that CS does eventually accumulate at the interface. We speculate that while AavLEA1 competes well with the initial association of native CS with the surface, some CS is still able to adsorb and denature. Once denatured, CS cannot be efficiently displaced by AavLEA1, due to higher surface activity of the denatured protein. Nor can the LEA protein act as a chaperone to sequester or aid refolding. Therefore, LEA proteins act as kinetic stabilisers, providing effective protection during short periods of stress, but over long periods are less effective.

The role of IDPs in stress tolerance continues to be an important area of scientific research. In this study, we have demonstrated that some IDPs have surface activity and propose this as a mechanism by which they

prevent the aggregation of sensitive globular proteins during the freeze–thaw process. These novel findings enhance our understanding of the biophysical and biochemical properties of IDPs in relation to their involvement in stress tolerance and may be of value in the development of novel biopreservation techniques.

### Abbreviations

CD, circular dichroism; CS, citrate synthase; D-AavLEA1, Deuterated AavLEA1; H-AavLEA1, hydrogenated AavLEA1; IDPs, intrinsically disordered proteins; ILL, Institut Laue-Langevin; IPTG, isopropyl- $\beta$ -D-thiogalactopyranoside; LEA, late embryogenesis abundant; MRE, mean residue ellipticities.

### Author Contribution

F.Y. and M.W. conducted, analysed, and interpreted all experiments, with help from A.F.R. on SANS and NR experiments. A.F.R. and A.T. supervised the project and provided input on the interpretation, design, and direction of the study. R.B. and F.Y. developed the new custom layer NR model and interpreted the NR data. F.Y. and M.W. drafted the manuscript and designed the figures. R.B., I.G., and R.K.H. provided guidance and training on NR and SANS techniques. All authors discussed the results and commented on the manuscript.

### Funding

F.Y. thanks the Natural Sciences and Engineering Research Council of Canada for a PhD scholarship. A.T. was supported by a European Research Council Advanced Investigator Grant 233232. The authors are grateful to the Rutherford laboratory and the ILL for the granting of beamtime. The ILL data may be found at <http://doi.ill.fr/10.5291/ILL-DATA.9-13-540n>.

### Competing Interests

The Authors declare that there are no competing interests associated with the manuscript.

### References

- 1 Tunnacliffe, A., Hincha, D.K., Leprince, O. and Macherel, D. (2010) LEA proteins: versatility of form and function. In *Dormancy and Resistance in Harsh Environments* (Lubzens, E., Cerda, J. and Clark, M., eds), pp. 91–108, Springer, Berlin
- 2 Hand, S.C., Menze, M.A., Toner, M., Boswell, L. and Moore, D. (2011) LEA proteins during water stress: not just for plants anymore. *Annu. Rev. Physiol.* **73**, 115–134 <https://doi.org/10.1146/annurev-physiol-012110-142203>
- 3 Battaglia, M., Olvera-Carrillo, Y., Garcarrubio, A., Campos, F. and Covarrubias, A.A. (2008) The enigmatic LEA proteins and other hydrophilins. *Plant Physiol.* **148**, 6–24 <https://doi.org/10.1104/pp.108.120725>
- 4 Jaspard, E., Macherel, D. and Hunault, G. (2012) Computational and statistical analyses of amino acid usage and physico-chemical properties of the twelve late embryogenesis abundant protein classes. *PLoS ONE* **7**, e36968 <https://doi.org/10.1371/journal.pone.0036968>
- 5 Koag, M.C., Fenton, R.D., Wilkens, S. and Close, T.J. (2003) The binding of maize DHN1 to lipid vesicles. Gain of structure and lipid specificity. *Plant Physiol.* **131**, 309–316 <https://doi.org/10.1104/pp.011171>
- 6 Alsheikh, M.K., Svensson, J.T. and Randall, S.K. (2005) Phosphorylation regulated ion-binding is a property shared by the acidic subclass dehydrins. *Plant Cell Environ.* **28**, 1114–1122 <https://doi.org/10.1111/j.1365-3040.2005.01348.x>
- 7 Chakrabortee, S., Tripathi, R., Watson, M., Schierle, G.S.K., Kurniawan, D.P., Kaminski, C.F. et al. (2012) Intrinsically disordered proteins as molecular shields. *Mol. Biosyst.* **8**, 210–219 <https://doi.org/10.1039/C1MB05263B>
- 8 Goyal, K., Walton, L.J. and Tunnacliffe, A. (2005) LEA proteins prevent protein aggregation due to water stress. *Biochem. J.* **388**, 151–157 <https://doi.org/10.1042/BJ20041931>
- 9 Chakrabortee, S., Boschetti, C., Walton, L.J., Sarkar, S., Rubinsztein, D.C. and Tunnacliffe, A. (2007) Hydrophilic protein associated with desiccation tolerance exhibits broad protein stabilization function. *Proc. Natl Acad. Sci. U.S.A.* **104**, 18073–18078 <https://doi.org/10.1073/pnas.0706964104>
- 10 Liu, Y., Chakrabortee, S., Li, R., Zheng, Y. and Tunnacliffe, A. (2011) Both plant and animal LEA proteins act as kinetic stabilisers of polyglutamine-dependent protein aggregation. *FEBS Lett.* **585**, 630–634 <https://doi.org/10.1016/j.febslet.2011.01.020>
- 11 Browne, J., Tunnacliffe, A. and Burnell, A. (2002) Anhydrobiosis – plant desiccation gene found in a nematode. *Nature* **416**, 38–38 <https://doi.org/10.1038/416038a>
- 12 Kiyosue, T., Yamaguchi-Shinozaki, K. and Shinozaki, K. (1994) Characterization of two cDNAs (ERD10 and ERD14) corresponding to genes that respond rapidly to dehydration stress in *Arabidopsis thaliana*. *Plant Cell Physiol.* **35**, 225–231 PMID:8069491
- 13 Goyal, K., Tisi, L., Basran, A., Browne, J., Burnell, A., Zurdo, J. et al. (2003) Transition from natively unfolded to folded state induced by desiccation in an anhydrobiotic nematode protein. *J. Biol. Chem.* **278**, 12977–12984 <https://doi.org/10.1074/jbc.M212007200>
- 14 Candat, A., Paszkiewicz, G., Neveu, M., Gautier, R., Logan, D.C., Avelange-Macherel, M.-H. et al. (2014) The ubiquitous distribution of late embryogenesis abundant proteins across cell compartments in *Arabidopsis* offers tailored protection against abiotic stress. *Plant Cell* **26**, 3148–3166 <https://doi.org/10.1105/tpc.114.127316>
- 15 Peränen, J., Rikkonen, M., Hyvönen, M. and Kääriäinen, L. (1996) T7 vectors with a modified T7lacPromoter for expression of proteins in *Escherichia coli*. *Anal. Biochem.* **236**, 371–373 <https://doi.org/10.1006/abio.1996.0187>
- 16 Bartsch, O. (1924) Über schaumssysteme. *Kolloid. Beihefte* **20**, 1–49 <https://doi.org/10.1007/BF02558490>

- 17 Whitmore, L. and Wallace, B.A. (2008) Protein secondary structure analyses from circular dichroism spectroscopy: methods and reference databases. *Biopolymers* **89**, 392–400 <https://doi.org/10.1002/bip.20853>
- 18 Provencher, S.W. and Gloeckner, J. (1981) Estimation of globular protein secondary structure from circular dichroism. *Biochemistry* **20**, 33–37 <https://doi.org/10.1021/bi00504a006>
- 19 van Stokkum, I.H.M., Spoelder, H.J.W., Bloemendal, M., van Grondelle, R. and Groen, F.C.A. (1990) Estimation of protein secondary structure and error analysis from circular dichroism spectra. *Anal. Biochem.* **191**, 110–118 [https://doi.org/10.1016/0003-2697\(90\)90396-Q](https://doi.org/10.1016/0003-2697(90)90396-Q)
- 20 Sreerama, N. and Woody, R.W. (2000) Estimation of protein secondary structure from circular dichroism spectra: comparison of CONTIN, SELCON, and CDSSTR methods with an expanded reference set. *Anal. Biochem.* **287**, 252–260 <https://doi.org/10.1006/abio.2000.4880>
- 21 Kolhe, P., Amend, E. and Singh, S.K. (2010) Impact of freezing on pH of buffered solutions and consequences for monoclonal antibody aggregation. *Biotechnol. Prog.* **26**, 727–733 <https://doi.org/10.1002/btpr.377>
- 22 Sreerama, N., Venyaminov, S.Y. and Woody, R.W. (1999) Estimation of the number of alpha-helical and beta-strand segments in proteins using circular dichroism spectroscopy. *Protein Sci.* **8**, 370–380 <https://doi.org/10.1110/ps.8.2.370>
- 23 Fisher, S.J. and Helliwell, J.R. (2008) An investigation into structural changes due to deuteration. *Acta Crystallogr. Sect. A: Found. Crystallogr.* **64**, 359–367 <https://doi.org/10.1107/S0108767308004807>
- 24 Dennison, S.R., Hauß, T., Dante, S., Brandenburg, K., Harris, F. and Phoenix, D.A. (2006) Deuteration can affect the conformational behaviour of amphiphilic  $\alpha$ -helical structures. *Biophys. Chem.* **119**, 115–120 <https://doi.org/10.1016/j.bpc.2005.09.002>
- 25 Chen, C.-H., Liu, I.W., MacColl, R. and Berns, D.S. (1983) Differences in structure and stability between normal and deuterated proteins (phycocyanin). *Biopolymers* **22**, 1223–1233 <https://doi.org/10.1002/bip.360220414>
- 26 Cecil, R. and Louis, C.F. (1970) Protein-hydrocarbon interactions. Interactions of various proteins with decane in the presence of alcohols. *Biochem. J.* **117**, 147–156 <https://doi.org/10.1042/bj1170147>
- 27 Macritchie, F. (1978) Proteins at interfaces. In *Advances in Protein Chemistry* (Anfinsen, C.B., Edsall, J.T. and Frederic, M.R., eds), pp. 283–326, Academic Press, New York
- 28 Maa, Y.-F. and Hsu, C.C. (1997) Protein denaturation by combined effect of shear and air-liquid interface. *Biotechnol. Bioeng.* **54**, 503–512 [https://doi.org/10.1002/\(SICI\)1097-0290\(19970620\)54:6<503::AID-BIT1>3.0.CO;2-N](https://doi.org/10.1002/(SICI)1097-0290(19970620)54:6<503::AID-BIT1>3.0.CO;2-N)
- 29 Wiesbauer, J., Prassl, R. and Nidetzky, B. (2013) Renewal of the air–water interface as a critical system parameter of protein stability: aggregation of the human growth hormone and its prevention by surface-active compounds. *Langmuir* **29**, 15240–15250 <https://doi.org/10.1021/la4028223>
- 30 Carte, A.E. (1961) Air bubbles in ice. *Proc. Phys. Soc.* **77**, 757 <https://doi.org/10.1088/0370-1328/77/3/327>
- 31 Kervin, B.A., Heller, M.C., Levin, S.H. and Randolph, T.W. (1998) Effects of tween 80 and sucrose on acute short-term stability and long-term storage at  $-20^{\circ}\text{C}$  of a recombinant hemoglobin. *J. Pharm. Sci.* **87**, 1062–1068 <https://doi.org/10.1021/js980140v>
- 32 Cao, E., Chen, Y., Cui, Z. and Foster, P.R. (2003) Effect of freezing and thawing rates on denaturation of proteins in aqueous solutions. *Biotechnol. Bioeng.* **82**, 684–690 <https://doi.org/10.1002/bit.10612>
- 33 Wu, H. and Liu, S.-. (1931) Coagulation of egg albumin by supersonic waves. *Proc. Soc. Exp. Biol. Med.* **28**, 782–784 <https://doi.org/10.3181/00379727-28-5532>
- 34 Miller, K.E., Skogerboe, K.J. and Synovec, R.E. (1999) Novel calibration of a dynamic surface tension detector: flow injection analysis of kinetically-hindered surface active analytes. *Talanta* **50**, 1045–1056 [https://doi.org/10.1016/S0039-9140\(99\)00210-6](https://doi.org/10.1016/S0039-9140(99)00210-6)
- 35 Krägel, J., Wüstneck, R., Husband, F., Wilde, P.J., Makievski, A.V., Grigoriev, D.O. et al. (1999) Properties of mixed protein/surfactant adsorption layers. *Colloids Surf. B. Biointerfaces* **12**, 399–407 [https://doi.org/10.1016/S0927-7765\(98\)00094-0](https://doi.org/10.1016/S0927-7765(98)00094-0)
- 36 Marinova, K.G., Bashaeva, E.S., Nenova, B., Temelska, M., Mirarefi, A.Y., Campbell, B. et al. (2009) Physico-chemical factors controlling the foamability and foam stability of milk proteins: sodium caseinate and whey protein concentrates. *Food Hydrocolloids* **23**, 1864–1876 <https://doi.org/10.1016/j.foodhyd.2009.03.003>
- 37 Mita, T., Ishida, E. and Matsumoto, H. (1978) Physicochemical studies on wheat protein foams. II. Relationship between bubble size and stability of foams prepared with gluten and gluten components. *J. Colloid Interface Sci.* **64**, 143–153 [https://doi.org/10.1016/0021-9797\(78\)90344-2](https://doi.org/10.1016/0021-9797(78)90344-2)
- 38 Cumper, C.W.N. (1953) The stabilization of foams by proteins. *Trans. Faraday Soc.* **49**, 1360–1369 <https://doi.org/10.1039/tf9534901360>
- 39 Dure, L. (1993) A repeating 11-mer amino acid motif and plant desiccation. *Plant J.* **3**, 363–369 <https://doi.org/10.1046/j.1365-313X.1993.101-19-00999.x>
- 40 Li, D. and He, X. (2009) Desiccation induced structural alterations in a 66-amino acid fragment of an anhydrobiotic nematode late embryogenesis abundant (LEA) protein. *Biomacromolecules* **10**, 1469–1477 <https://doi.org/10.1021/bm9002688>
- 41 Augenstine, L.G. and Ray, B.R. (1957) Trypsin monolayers at the air–water interface. III. Structural postulates on inactivation. *J. Phys. Chem.* **61**, 1385–1388 <https://doi.org/10.1021/j150556a028>
- 42 Donaldson, T.L., Boonstra, E.F. and Hammond, J.M. (1980) Kinetics of protein denaturation at gas–liquid interfaces. *J. Colloid Interface Sci.* **74**, 441–450 [https://doi.org/10.1016/0021-9797\(80\)90213-1](https://doi.org/10.1016/0021-9797(80)90213-1)
- 43 Dill, K.A. (1990) Dominant forces in protein folding. *Biochemistry* **29**, 7133–7155 <https://doi.org/10.1021/bi00483a001>
- 44 Rey, L. (2010) *Freeze-Drying/Lyophilization of Pharmaceutical and Biological Products*, 3rd edn, CRC Press
- 45 Schwegman, J.J., Carpenter, J.F. and Nail, S.L. (2009) Evidence of partial unfolding of proteins at the ice/freezing-concentrate interface by infrared microscopy. *J. Pharm. Sci.* **98**, 3239–3246 <https://doi.org/10.1002/jps.21843>
- 46 Krieglgaard, L., Jones, L.S., Randolph, T.W., Frokjaer, S., Flink, J.M., Manning, M.C. et al. (1998) Effect of Tween 20 on freeze-thawing- and agitation-induced aggregation of recombinant Human Factor XIII. *J. Pharm. Sci.* **87**, 1597–1603 <https://doi.org/10.1021/js980126i>
- 47 Cordes, A.A., Carpenter, J.F. and Randolph, T.W. (2012) Accelerated stability studies of abatacept formulations: comparison of freeze–thawing- and agitation-induced stresses. *J. Pharm. Sci.* **101**, 2307–2315 <https://doi.org/10.1002/jps.23150>
- 48 Sasaki, K., Christov, N.K., Tsuda, S. and Imai, R. (2013) Identification of a novel LEA protein involved in freezing tolerance in wheat. *Plant Cell Physiol.* **55**, 136–147 <https://doi.org/10.1093/pcp/pct164>
- 49 Hanin, M., Brini, F., Ebel, C., Toda, Y., Takeda, S. and Masmoudi, K. (2011) Plant dehydrins and stress tolerance: versatile proteins for complex mechanisms. *Plant Signal. Behav.* **6**, 1503–1509 <https://doi.org/10.4161/psb.6.10.17088>

- 50 Honjoh, K., Matsumoto, H., Shimizu, H., Ooyama, K., Tanaka, K., Oda, Y. et al. (2000) Cryoprotective activities of Group 3 late embryogenesis abundant proteins from *Chlorella vulgaris* C-27. *Biosci. Biotechnol. Biochem.* **64**, 1656–1663 <https://doi.org/10.1271/bbb.64.1656>
- 51 Akram, M.S. (2013) Functionalised self-assembling polyglutamine fusion tags. In *Department of Chemical Engineering and Biochemistry*, University of Cambridge, Cambridge, U.K.
- 52 Lee, C.F., Bird, S., Shaw, M., Jean, L. and Vaux, D.J. (2012) Combined effects of agitation, macromolecular crowding, and interfaces on amyloidogenesis. *J. Biol. Chem.* **287**, 38006–38019 <https://doi.org/10.1074/jbc.M112.400580>
- 53 Thalhammer, A., Bryant, G., Sulpice, R. and Hinch, D.K. (2014) Disordered cold regulated 15 proteins protect chloroplast membranes during freezing through binding and folding, but do not stabilize chloroplast enzymes *in vivo*. *Plant Physiol.* **166**, 190–201 <https://doi.org/10.1104/pp.114.245399>
- 54 Tolleter, D., Hinch, D.K. and Macherel, D. (2010) A mitochondrial late embryogenesis abundant protein stabilizes model membranes in the dry state. *Biochim. Biophys. Acta* **1798**, 1926–1933 <https://doi.org/10.1016/j.bbamem.2010.06.029>
- 55 Segrest, J.P., Jones, M.K., De Loof, H., Brouillette, C.G., Venkatachalapathi, Y.V. and Anantharamaiah, G.M. (1992) The amphipathic helix in the exchangeable apolipoproteins: a review of secondary structure and function. *J. Lipid Res.* **33**, 141–166 PMID:1569369
- 56 Segrest, J.P., De Loof, H., Dohlman, J.G., Brouillette, C.G. and Anantharamaiah, G.M. (1990) Amphipathic helix motif: classes and properties. *Proteins Struct. Funct. Bioinformatics* **8**, 103–117 <https://doi.org/10.1002/prot.340080202>
- 57 Bremer, A., Kent, B., Hauß, T., Thalhammer, A., Yepuri, N.R., Darwish, T.A. et al. (2017) Intrinsically disordered stress protein COR15A resides at the membrane surface during dehydration. *Biophys. J.* **113**, 572–579 <https://doi.org/10.1016/j.bpj.2017.06.027>
- 58 Vroman, L., Adams, A., Fischer, G. and Munoz, P. (1980) Interaction of high molecular weight kininogen, factor XII, and fibrinogen in plasma at interfaces. *Blood* **55**, 156–159 PMID:7350935
- 59 Slack, S. M. and Horbett, T. A. (1995) The Vroman effect. In *Proteins at Interfaces II* (Horbett, T.A. and Brash, J.L., eds), pp. 112–128, American Chemical Society, Washington

## Supplementary information

A custom layer approach was written to be used in conjunction with RASCAL to describe systems where there are no standard discrete layers. The code used is copied below and can be adapted for various multi-component systems.

```
function output = AdsorptionPchip(params,bulk_in,bulk_out,contrast)

%Setting Bulk Values
st_val = bulk_in(contrast);
end_val = bulk_out(contrast);

%Defining Parameters
range = params(1);
n_points = (length(params)-1)/2;

%Making Layers
xx = 0:range;
step = range/(n_points+1);
x = [0:step:range];
PercentProtein1 = params(2:(n_points+1));
PercentProtein2 = params((n_points+2):end);
end

SLD = ((PercentProtein1*Protein1_SLD) +
(PercentProtein2*Protein2_SLD) + ((100-(PercentProtein1 +
PercentProtein2))*bulk_out(contrast)))/100;
y_column = SLD(:);
y = [st_val ; y_column ; end_val];
yy = pchip(x,y,xx);

output = [xx(:) yy(:)];
```

*Table S1: Chi-squared values calculated from fitting neutron reflection data*

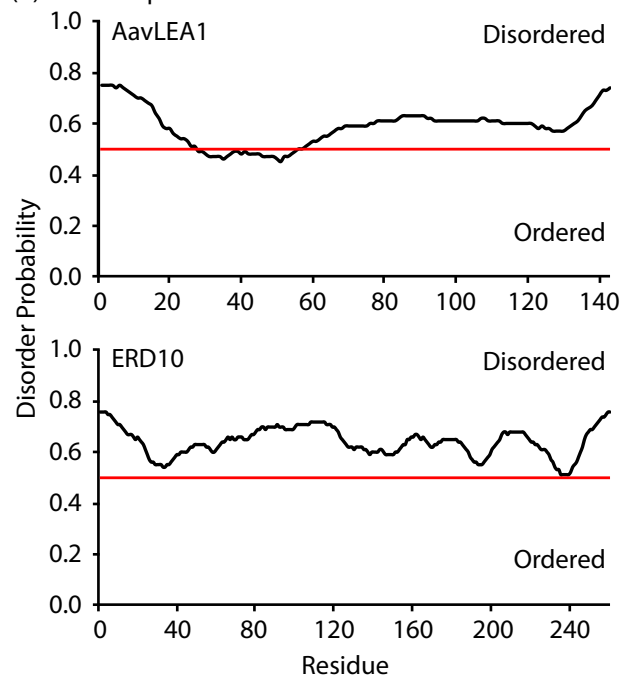
<b>Data Set</b>	<b>Chi-Squared</b>
CS	79.4
LEA	330.9
CS + LEA @ 30 s	5.7
CS + LEA @ 1 min	17.3
CS + LEA @ 5 min	14.9
CS + LEA @ 30 min	11.3
CS + LEA @ 60 min	10.0
CS + LEA @ 2 h	715.1



(a) Amino acid usage

		AavLEA1		ERD10	
		n	%	n	%
Hydrophobic (aliphatic)	A	19	13.29	9	3.46
	C	0	0.00	0	0.00
	M	5	3.50	6	2.31
	V	3	2.10	16	6.15
	L	4	2.80	12	4.62
Hydrophobic (aromatic)	I	1	0.70	8	3.08
	Y	2	1.40	2	0.77
	W	1	0.70	0	0.00
Polar	F	2	1.40	7	2.69
	S	6	4.20	18	6.92
	T	9	6.29	17	6.54
	N	4	2.80	5	1.92
Acidic	Q	17	11.89	7	2.69
	D	5	3.50	14	5.38
Basic	E	25	17.48	51	19.62
	H	1	0.70	11	4.23
	K	17	11.89	42	16.15
Other	R	9	6.29	3	1.15
	G	13	9.09	13	5.00
	P	0	0.00	19	7.31

(b) Disorder prediction



(c) Sequence motifs

AavLEA1 (143 aa)

MSSQQNQNRQGEQQEQGYMEAAKEKVVNAWESTKETLSSTAQAAAEEKTAEFRDSAGETIRDLTGQAQEKG  
QEFKERAGEKAEETKORAGEKMDETKORAGEMRENAGQKMEEYKQQGKGKAEELRDTAAEKLHQAGEKVK  
GRD

ERD10 (260 aa)

MAEYKNTVPEQETPKVATEESSAPEIKERGMDFDLKKKEEVKPKQETTTLASEFEHKTQISEPESFVAKH  
EEEEHKPTLLEQLHQKHEEEENKPSLLDKLHRSNSSSSSSDEEGEDGEKKKKEKKKIVEGDHVKTVE  
EENQGVMDRIKEKFPPLGEKPGDDVPVVTMPAPHSVEDHKPEEEKKGFMDKIKEKLPCHSKKPEDSQV  
VNTTPLVETATPIADIPEKKGFMDKIKEKLPGYHAKTTGEEKKEKVS

**Figure S1:** Sequence properties of the two LEA proteins used in this study (a) Amino acid composition of AavLEA1 and ERD10. (b) Consensus disorder predictions from metaPrDOS (<http://prdos.hgc.jp/meta/>)<sup>1</sup> (c) Amino acid sequences for AavLEA1 highlighting the 4 copies of the 11mer consensus motif and ERD10 indicating the 2 copies of the K segment (red) and the S segment (yellow).

**Supplementary references**

1. Ishida, T. and Kinoshita, K. Prediction of disordered regions in proteins based on the meta approach. *Bioinformatics*. **24**, 1344-1348